

# METAL-ORGANIC FRAMEWORKS

---

## Design and Application

Edited by

LEONARD R. MACGILLIVRAY

University of Iowa



WILEY

A JOHN WILEY & SONS, INC., PUBLICATION



# **METAL-ORGANIC FRAMEWORKS**



# METAL-ORGANIC FRAMEWORKS

---

## Design and Application

Edited by

LEONARD R. MACGILLIVRAY

University of Iowa



WILEY

A JOHN WILEY & SONS, INC., PUBLICATION

Copyright © 2010 by John Wiley & Sons, Inc. All rights reserved.

Published by John Wiley & Sons, Inc., Hoboken, New Jersey

Published simultaneously in Canada

No part of this publication may be reproduced, stored in a retrieval system, or transmitted in any form or by any means, electronic, mechanical, photocopying, recording, scanning, or otherwise, except as permitted under Section 107 or 108 of the 1976 United States Copyright Act, without either the prior written permission of the Publisher, or authorization through payment of the appropriate per-copy fee to the Copyright Clearance Center, Inc., 222 Rosewood Drive, Danvers, MA 01923, 978-750-8400, fax 978-750-4470, or on the web at [www.copyright.com](http://www.copyright.com). Requests to the Publisher for permission should be addressed to the Permissions Department, John Wiley & Sons, Inc., 111 River Street, Hoboken, NJ 07030, 201-748-6011, fax 201-748-6008, or online at <http://www.wiley.com/go/permission>.

**Limit of Liability/Disclaimer of Warranty:** While the publisher and author have used their best efforts in preparing this book, they make no representations or warranties with respect to the accuracy or completeness of the contents of this book and specifically disclaim any implied warranties of merchantability or fitness for a particular purpose. No warranty may be created or extended by sales representatives or written sales materials. The advice and strategies contained herein may not be suitable for your situation. You should consult with a professional where appropriate. Neither the publisher nor author shall be liable for any loss of profit or any other commercial damages, including but not limited to special, incidental, consequential, or other damages.

For general information on our other products and services or for technical support, please contact our Customer Care Department within the United States at 800-762-2974, outside the United States at 317-572-3993 or fax 317-572-4002.

Wiley also publishes its books in a variety of electronic formats. Some content that appears in print may not be available in electronic formats. For more information about Wiley products, visit our web site at [www.wiley.com](http://www.wiley.com).

***Library of Congress Cataloging-in-Publication Data:***

Metal-organic frameworks: design and application / edited by Leonard R. MacGillivray.

p. cm.

Includes index.

ISBN 978-0-470-19556-7 (cloth)

1. Supramolecular organometallic chemistry. 2. Organometallic polymers. 3. Porous materials. I. MacGillivray, Leonard R.

QD882.M48 2010

547'.0504426-dc22

2009049259

Printed in Singapore

10 9 8 7 6 5 4 3 2 1

# CONTENTS

<b>Preface</b>	<b>vii</b>
<b>Contributors</b>	<b>xi</b>
<b>1 From Hofmann Complexes to Organic Coordination Networks</b>	<b>1</b>
<i>Makoto Fujita</i>	
<b>2 Insight into the Development of Metal-Organic Materials (MOMs): At Zeolite-like Metal-Organic Frameworks (ZMOFs)</b>	<b>37</b>
<i>Mohamed Eddaoudi and Jarrod F. Eubank</i>	
<b>3 Topology and Interpenetration</b>	<b>91</b>
<i>Stuart R. Batten</i>	
<b>4 Highly Connected Metal-Organic Frameworks</b>	<b>131</b>
<i>Peter Hubberstey, Xiang Lin, Neil R. Champness, and Martin Schröder</i>	
<b>5 Surface Pore Engineering of Porous Coordination Polymers</b>	<b>165</b>
<i>Sujit K. Ghosh and Susuma Kitagawa</i>	
<b>6 Rational Design of Non-centrosymmetric Metal-Organic Frameworks for Second-Order Nonlinear Optics</b>	<b>193</b>
<i>Wenbin Lin and Shuting Wu</i>	
<b>7 Selective Sorption of Gases and Vapors in Metal-Organic Frameworks</b>	<b>215</b>
<i>Hyunuk Kim, Hyungphil Chun, and Kimoon Kim</i>	

<b>8</b>	<b>Hydrogen and Methane Storage in Metal-Organic Frameworks</b>	<b>249</b>
	<i>David J. Collins, Shengqian Ma, and Hong-Cai Zhou</i>	
<b>9</b>	<b>Towards Mechanochemical Synthesis of Metal-Organic Frameworks: From Coordination Polymers and Lattice Inclusion Compounds to Porous Materials</b>	<b>267</b>
	<i>Tomislav Friščić</i>	
<b>10</b>	<b>Metal-Organic Frameworks with Photochemical Building Units</b>	<b>301</b>
	<i>Saikat Dutta, Ivan G. Georgiev, and Leonard R. MacGillivray</i>	
<b>11</b>	<b>Molecular Modeling of Adsorption and Diffusion in Metal-Organic Frameworks</b>	<b>313</b>
	<i>Randall Q. Snurr, A. Özgür Yazaydin, David Dubbeldam, and Houston Frost</i>	
	<b>Index</b>	<b>341</b>



# PREFACE

The field of metal-organic frameworks, or MOFs, is undergoing accelerated and sustained growth. I personally became acquainted with MOFs, or more generally coordination polymers, as an undergraduate research student while at Saint Mary's University, Halifax, Nova Scotia, Canada, from 1991 to 1994. The process of mixing readily available metal precursors with organic linkers—many of which fell under the heading of being commercially available—to produce a wide array of extended frameworks clearly then, and now, captured the imagination of chemists and materials scientists worldwide.

From a fundamental standpoint, there is an important link between MOF chemistry and the field of inorganic chemistry. In many ways, MOF chemistry enables chemists to connect previously existing coordination complexes so as to make a conceptual link into the field of materials chemistry. This link has now evolved to afford applications ranging from catalysis to energy storage. Organic chemists are also able to contribute to the mix by crafting ligands with properties that one ultimately plans to express within the walls of MOFs. Solid-state chemists and X-ray crystallographers provide insights into the structures of MOFs so that the process of designing and synthesizing MOFs can be refined so as to ultimately control a targeted property and give rise to function.

My personal draw to MOFs was, in retrospect, also inspired by the field of supramolecular chemistry, particularly as it relates to the rational design of solids, or crystal engineering. The early 1990s witnessed supramolecular chemistry envelop the process of self-assembly, with a crystal being regarded as a supermolecule par excellence.<sup>1</sup> Metal–ligand bonding is reversible and, thus, fits within the realm of supramolecular chemistry. Self-assembly involves subunits of a larger superstructure

being repeated in zero-dimensional (0D), 1D, 2D, or 3D space, with the solid state being a perfect resting place for intermolecular forces to dominate. Today, many of the boundaries between these areas have become increasingly more difficult to distinguish, which can be expected as more is being uncovered and as more emphasis is placed on properties and function.

It is, thus, with great pleasure that I am able to assemble a multi-author monograph that includes authoritative contributions from leading research laboratories in the field of MOF chemistry. My goal is to provide insights into where the field of MOFs began to take root and provide an account of the fundamentals that define where the field has come and is able to go. Indeed, MOFs provide chemists a means to think about how to utilize coordination space to mimic the chemistry of zeolites with an added degree of organic function. These possibilities have become apparent in key developments and important advances that are outlined in the chapters that follow.

Fujita (Chapter 1) and Eddaoudi (Chapter 2), for example, document the first reports of MOFs, or coordination networks, particularly those that exhibit catalysis, the emergence of heteroaromatic ligands, and how carboxylates provided an important entry to increasingly robust solids. Batten (Chapter 3) demonstrates a role of symmetry in defining and understanding the simple and complex frameworks that result from the solid-state assembly process that affords a MOF. Next, Schroder (Chapter 4) addresses the design and synthesis of extended frameworks of increasingly structural complexity in the form of highly connected MOFs based on lanthanide ions. Kitagawa (Chapter 5) then shows how the internal structures of coordination networks can be rationally modified and tailored with organic groups while Lin (Chapter 6) documents some of the first systematic applications of MOFs as they relate to the generation of nonlinear optic materials. A great challenge facing mankind is making efficient use of energy. MOFs have emerged as potentially useful platforms for facing this challenge in the form of gas storage, separation, and conversion. Thus, Kim (Chapter 7) and Zhou (Chapter 8) address how MOFs interact with small gas molecules (e.g.,  $H_2$ ) and how these materials may be integrated into schemes for energy utilization. In a related topic, Friscic (Chapter 9) tackles the emerging issue of mechanochemical, or solvent-free, “green” preparation of MOFs while work by our group demonstrates how the walls of extended frameworks can be designed to serve as platforms for light-induced chemical reactions (Chapter 10). Finally, Snurr (Chapter 11) addresses how the field of computational chemistry can be used to understand, and ultimately, aid the design of MOFs, with targeted applications in separations, gas uptake, and materials characterization. Carefully chosen references serve to guide the reader through the extensive literature, which makes the field accessible to a wide and varied audience.

My initial interests in the chemistry of MOFs, and supramolecular chemistry and solid-state chemistry in general, stemmed from an experience as an undergraduate researcher. It is for this reason that I dedicate this monograph to the

undergraduate research experience and to all of those that support undergraduate research.

LEONARD R. MACGILLIVRAY

*Iowa City, IA*

*March 2010*

## REFERENCE

- 1 Dunitz, J. D. *Pure Appl. Chem.* **1991**, *63*, 177.



# CONTRIBUTORS

**Stuart R. Batten**, School of Chemistry, Clayton Campus, Bldg. 19, Monash University, 3800 Australia

**Neil R. Champness**, School of Chemistry, The University of Nottingham, University Park, Nottingham, NG7 2RD, UK

**Hyungphil Chun**, Department of Applied Chemistry, College of Science and Technology, Hanyang University, 1271 Sadong, Ansan 426-791, Republic of Korea

**David J. Collins**, Department of Chemistry and Biochemistry, Miami University, Oxford, OH 45056, USA; Department of Chemistry, Texas A&M University, College Station, TX 77843, USA

**David Dubbeldam**, Department of Chemical and Biological Engineering, Northwestern University, 2145 Sheridan Road E136, Evanston, IL 60208, USA

**Saikat Dutta**, Department of Chemistry, University of Iowa, Iowa City, IA 52242, USA

**Mohamed Eddaoudi**, Department of Chemistry, University of South Florida, 4202 East Fowler Avenue, CHE204, Tampa, FL 33620, USA

**Jarrod F. Eubank**, Department of Chemistry, University of South Florida, 4202 East Fowler Avenue, CHE204, Tampa, FL 33620, USA

**Tomislav Friščić**, Department of Chemistry, University of Cambridge, Lensfield Road, Cambridge CB2 1EW, UK

**Houston Frost**, Department of Chemical and Biological Engineering, Northwestern University, 2145 Sheridan Road E136, Evanston, IL 60208, USA

**Makoto Fujita**, Department of Applied Chemistry, School of Engineering, University of Tokyo, 7-3-1 Hongo, Bunkyo-ku, Tokyo, 113-8656, Japan

**Ivan G. Georgiev**, Department of Chemistry, University of Iowa, Iowa City, IA 52242, USA

**Sujit K. Ghosh**, Department of Synthetic Chemistry and Biological Chemistry, Graduate School of Engineering, Kyoto University, Nishikyo-ku, Kyoto 615-8510, Japan; Department of Chemistry, Indian Institute of Science Education and Research (IISER), Pune, India

**Peter Hubberstey**, School of Chemistry, The University of Nottingham, University Park, Nottingham, NG7 2RD, UK

**Hyunuk Kim**, National Creative Research Initiative Center for Smart Supramolecules, Department of Chemistry and Division of Advanced Materials Science, Pohang University of Science and Technology, Pohang, 790-784, Republic of Korea

**Kimoon Kim**, National Creative Research Initiative Center for Smart Supramolecules, Department of Chemistry and Division of Advanced Materials Science, Pohang University of Science and Technology, Pohang, 790-784, Republic of Korea

**Susumu Kitagawa**, Department of Synthetic Chemistry and Biological Chemistry, Graduate School of Engineering, Kyoto University, Nishikyo-ku, Kyoto 615-851 Japan; Kitagawa Integrated Pore Project, Exploratory Research for Advanced Technology (ERATO), Japan Science and Technology Agency (JST), Shimogyo-ku, Kyoto 600-8815, Japan; Institute for Cell Materials Sciences (iCeMS), Kyoto University, Sokyo-ku, Kyoto, Japan

**Wenbin Lin**, Department of Chemistry, CB3290, University of North Carolina at Chapel Hill, Chapel Hill, NC 27599, USA

**Xiang Lin**, School of Chemistry, The University of Nottingham, University Park, Nottingham, NG7 2RD, UK

**Shengqian Ma**, Department of Chemistry and Biochemistry, Miami University, Oxford, OH 45056, USA; Department of Chemistry, Texas A&M University, College Station, TX 77843, USA

**Leonard R. MacGillivray**, Department of Chemistry, University of Iowa, Iowa City, IA 52242, USA

**Martin Schröder**, School of Chemistry, The University of Nottingham, University Park, Nottingham, NG7 2RD, UK

**Randall Q. Snurr**, Department of Chemical and Biological Engineering, Northwestern University, 2145 Sheridan Road E136, Evanston, IL 60208, USA

**A. Özgür Yazaydin**, Department of Chemical and Biological Engineering, Northwestern University, 2145 Sheridan Road E136, Evanston, IL 60208, USA

**Shuting Wu**, Department of Chemistry, CB3290, University of North Carolina at Chapel Hill, Chapel Hill, NC 27599, USA

**Hong-Cai Zhou**, Department of Chemistry and Biochemistry, Miami University, Oxford, OH 45056, USA; Department of Chemistry, Texas A&M University, College Station, TX 77843, USA

---

# 1

---

## FROM HOFMANN COMPLEXES TO ORGANIC COORDINATION NETWORKS

MAKOTO FUJITA

*Department of Applied Chemistry, School of Engineering, University of Tokyo,  
7-3-1 Hongo, Bunkyo-ku, Tokyo 113-8656, Japan*

### 1.1 INTRODUCTION

Recently, there has been a considerable upsurge in the study of porous hybrid organic–inorganic materials referred as *organic coordination networks*. Porous organic coordination networks can be prepared via self-assembly of a connector (a metal) and a link (a ligand) where connectors and ligands are bound together through a metal–ligand bond to form porous crystalline structures. It is in the pores that a wide range of processes can be carried out. One salient feature of coordination networks is the possibility to *design* the pores. Now it is possible to create pores with determined sizes just by selecting ligands with determined shapes, and particular environments through functionalization of the ligands. Therefore, certain reactions that are not possible to be carried out in solution are now being carried out within the porous space.

Another feature of organic coordination networks is their flexibility, which differentiates them from the robust frameworks of zeolites. This flexibility enables a dynamic behavior in porous coordination networks, which facilitate structural modifications (guest exchange or chemical reactions within the pores) without loss of its structural integrity. Hence, chemical reactions that occur in the pore can be monitored *in situ* in great detail by X-ray crystallography and other spectroscopic techniques.

The growing interest in such materials both scientifically and economically is not surprising due to the remarkable physicochemical properties that have been reported during the last two decades. Organic coordination networks are useful in a wide range of applications. For instance, these porous networks can be used in processes such as selective separation, catalytic reactions, guest exchange, and gas storage. Thus, due to its importance, in this review we have summarized the history of the coordination networks from the first documented examples until the latest advances in this field.

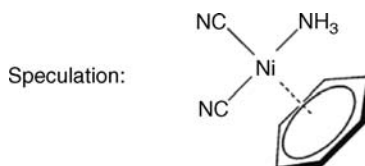
## 1.2 DISCOVERY OF A COORDINATION NETWORK

Initially porous and open-framework coordination networks attracted considerable attention as post-zeolite materials. Recent progresses of coordination networks are remarkable in that many intriguing properties and functions, for example robust and flexible framework, framework transformation, pore post-modification, selective molecular recognition, gas adsorption, and catalysis, have been reported. This review follows the history of coordination networks from the beginning, namely, Hofmann complex.

### 1.2.1 Hofmann Complex

The first coordination network having a chemical formula of  $\text{Ni}(\text{CN})_2(\text{NH}_3)\cdot\text{C}_6\text{H}_6$  was discovered by Hofmann and Küspert in 1897.<sup>1</sup> They obtained the complex as a crystal by slow layering diffusion of  $\text{C}_6\text{H}_6$  into an  $\text{NH}_3$  solution of  $\text{Ni}(\text{CN})_2$ . Pfeiffer in 1927<sup>2</sup> and Feigl in 1944<sup>3</sup> speculated that the structure of Hofmann complex was a Ni monomer coordinated by benzene as a side-on form,  $\text{Ni}(\text{CN})_2(\text{NH}_3)(\eta^6\text{-C}_6\text{H}_6)$  (Scheme 1.1).

Finally in 1954 Powell and coworkers clarified the structure of the Hofmann complex by X-ray analysis (unit cell dimensions  $a = b = 7.242 \text{ \AA}$ ;  $c = 8.277 \text{ \AA}$ <sup>3</sup>;  $\alpha = \beta = \gamma = 90$ ). The crystal structure was a square network bridged by CN groups encapsulating benzene in a channel.<sup>4</sup> A partial structure of the Hofmann complex is shown in Figure 1.1. Arrays of Ni covalently linked through CN groups form two-dimensional layers that are parallel to each other. From each layer two amine groups protrude toward the adjacent layer, creating a series of voids where benzene molecules are included.



SCHEME 1.1



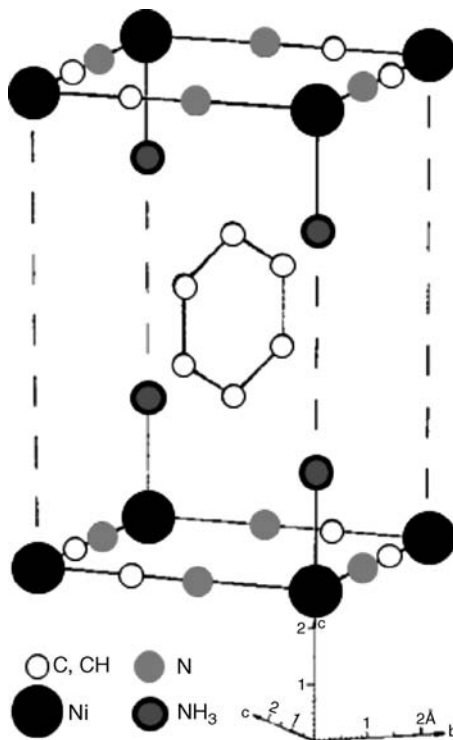
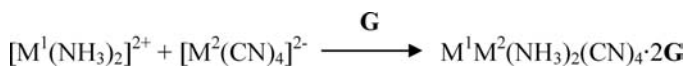


**FIGURE 1.1** A partial crystal structure of the Hoffman complex showing benzene encapsulation within the cavity.

### 1.2.2 Variation of the Hofmann Complex

Thereafter various Hofmann type complexes have been reported. Iwamoto and coworkers reported  $M^1M^2(NH_3)_2(CN)_4 \times G$  ( $M^1$ : Ni, Zn, Cd, Cu, Mn, Fe, Co;  $M^2$ : Ni, Pd, Pt;  $G$ : benzene, aniline, pyrrole, thiophene) in 1967–1968.<sup>5,6</sup> They paid attention to the components of Hofmann complex that can be divided into three parts:  $[Ni(NH_3)_2]^{2+} + [Ni(CN)_4]^{2-} + 2C_6H_6$ . Therefore, they prepared Hofmann type complexes according to the following Scheme 1.2. The structures were identified by powder X-ray diffraction analysis.

Walker and Hawthorne proposed expanded *n*-alkylamine Hofmann complexes in 1966 (Figure 1.2).<sup>7</sup> The complexes were synthesized by addition of *n*-alkylamines to a suspension to anhydrous nickel cyanide (Scheme 1.3). The crystalline samples were studied using the powder X-ray diffraction technique.



**SCHEME 1.2**

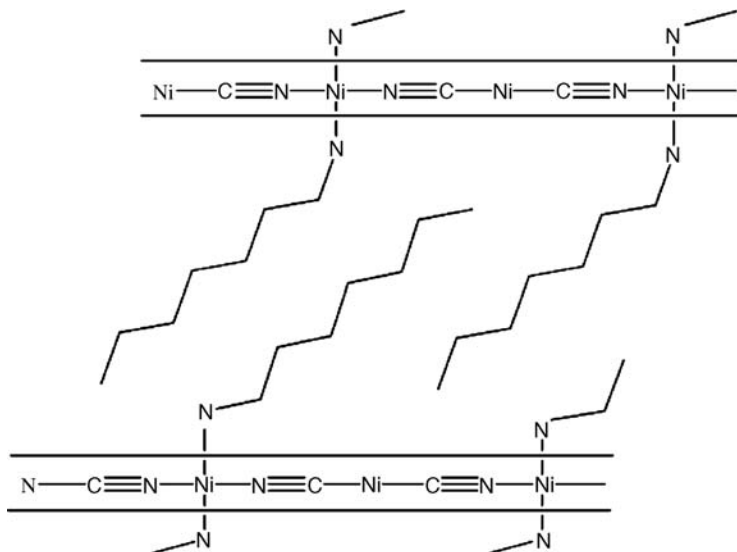
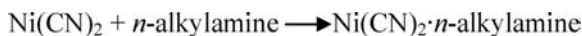


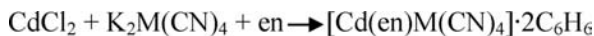
**FIGURE 1.2** Proposed structure of the expanded Hofmann complexes using *n*-alkylamines.

In 1968–1975, Iwamoto and coworkers also reported expanded Hofmann complexes bridged by ethylenediamine (en)<sup>8</sup> (Scheme 1.4). The structure was determined by X-ray analysis (Figure 1.3). The coordination network can encapsulate aromatic guests such as aniline, benzene, thiophene, and pyrrole.

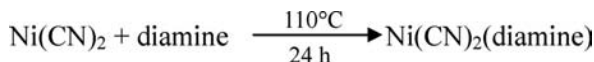
In 1977, Mathey prepared aromatic diamine complexes as shown in Scheme 1.5.<sup>9</sup> Depending on the length of diamines, the length of the *c*-axis also varies (Figure 1.4). The diamine complexes show selective encapsulation for aromatic guests and solvents. For example, [Ni(4,4'-bipyridyl)Ni(CN)<sub>4</sub>] encapsulate 0.8G (G: benzene, naphthalene, anthracene, CHCl<sub>3</sub>, CH<sub>2</sub>Cl<sub>2</sub>, CH<sub>3</sub>OH, but not phenanthrene, CCl<sub>4</sub>).



**SCHEME 1.3**



**SCHEME 1.4**



**SCHEME 1.5**

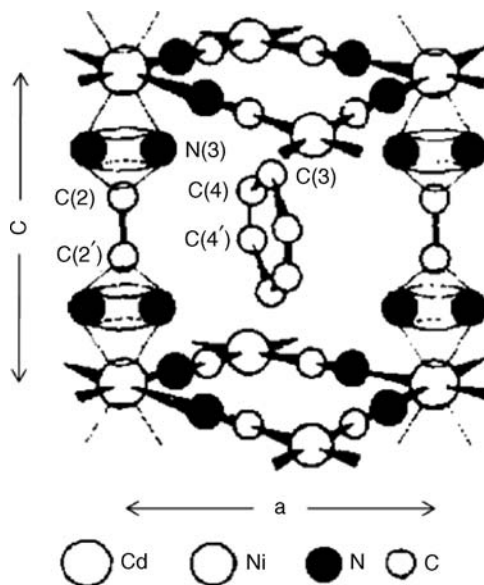


FIGURE 1.3 Representation of  $[\text{Cd}(\text{en})\text{Ni}(\text{CN})_4] \cdot 2\text{C}_6\text{H}_6$ .

Likewise Iwamoto and coworkers expanded from Hofmann complex into 1,2-diaminopropane (pn) complex in 1980,<sup>10</sup> dimethylamine complex in 1982–1984,<sup>11</sup> and 1, $\omega$ -diaminoalkane complex (1, $\omega$ -diaminoalkane:  $\text{H}_2\text{N}(\text{CH}_2)_n\text{NH}_2$ ,  $n = 4-8$ ) in 1984–1985.<sup>12</sup> Each complex encapsulated specific aromatic compounds. In addition, they prepared many related complexes by combination of metal ions with bridging ligands.<sup>13</sup>

As a whole, Iwamoto and colleagues developed unique chemistry of intriguing series of Hofmann complexes. He is one of pioneers to show promising future visions of designable coordination networks as a new class of materials.

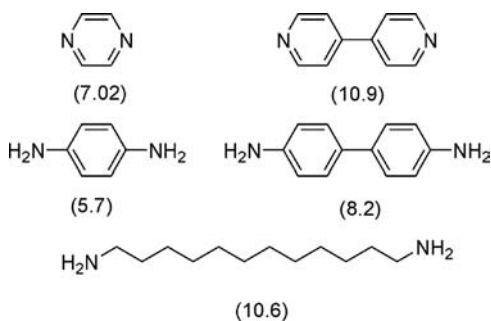


FIGURE 1.4 Diamines and  $c$ -axis values (in parentheses, Å).

### 1.3 ORGANIC COORDINATION NETWORK: ORGANIC MODIFICATION OF THE HOFMANN COMPLEX

Hofmann complex inspired scientists to develop strategies aiming to find a new class of materials. Worldwide the effort of many researchers paved the way for finding a new route to synthesize materials having larger cavities. For instance, if a  $-\text{CN}$  group could be replaced with organic linkers, a variety of coordination networks having finely tuned cavities could be prepared.

#### 1.3.1 Organic Coordination Network: The First Example

In 1989, Robson reported the first organic coordination network by complexation of anions with tetrahedral bridging ligands.<sup>14</sup> The aim of their work was to prepare three-dimensional solid polymeric materials with cavities by linking centers together with either a tetrahedral or an octahedral array of valencies. They prepared an infinite framework  $\{\text{Cu}^{\text{I}}[\text{C}(\text{C}_6\text{H}_4\text{-CN}_4)]\}^+$  of tetrahedral centers linked together by rod-like units. The rod-like units were obtained by substitution of the acetonitrile ligands in  $[\text{Cu}^{\text{I}}(\text{CH}_3\text{CN})_4]^+$  by 4,4',4'',4-tetracyanotetraphenylmethane.

X-ray crystallographic analysis revealed a diamond-like structure containing disordered nitrobenzene and  $\text{BF}_4^-$  ions in the cavities (Figure 1.5). The framework has adamantane-like cavities with a volume of approximately  $700 \text{ \AA}^3$ . It was estimated

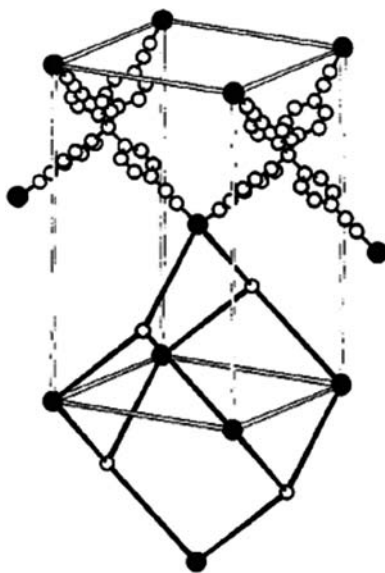


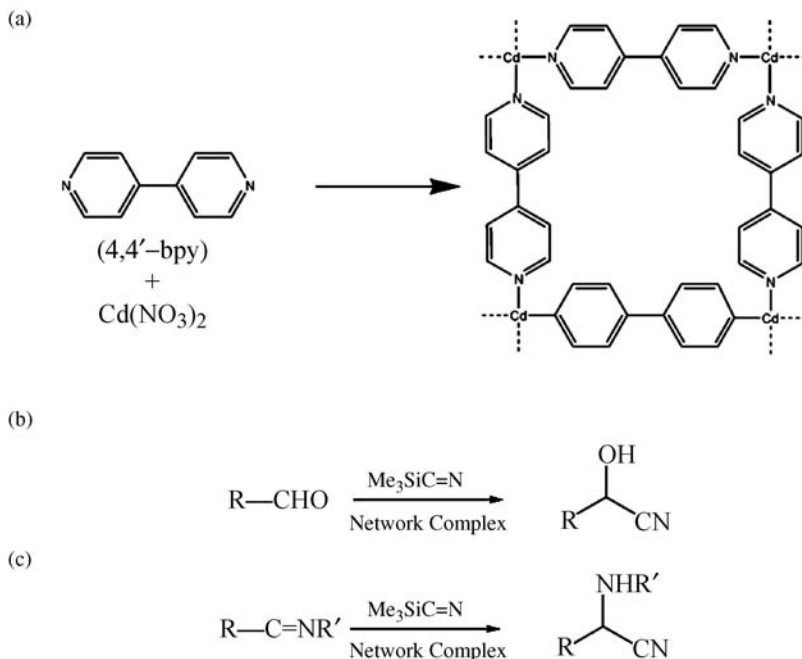
**FIGURE 1.5** Tetragonal unit cell with parts of adjacent unit cells of  $\{\text{Cu}^{\text{I}}[\text{C}(\text{C}_6\text{H}_4\text{-CN}_4)]\}^+$ . Gray circles denote the Cu atoms. The adamantane-like cavity is highlighted (black sticks). Nitrobenzene molecules and  $\text{BF}_4^-$  are omitted for clarity.

that the framework represents one third of the volume of the crystal while the remaining two thirds correspond to the nitrobenzene and  $\text{BF}_4^-$  ions.

With this work Robson and coworkers established a new strategy capable of designing new solids containing large cavities by linking organic molecules with determined size and shape.

#### 1.4 M-BIPYRIDINE SQUARE GRIDS: TWO-WAY LINK. TOWARD NEW FUNCTIONS AND APPLICATIONS OF ORGANIC COORDINATION NETWORKS

The preparation of a macrocyclic polynuclear complex  $[(\text{en})\text{Pd}(4,4'\text{-bpy})]_4(\text{NO}_3)_8$  (bpy = bipyridine) with the ability to recognize organic molecules in aqueous environment was an important step toward the applicability of such organic coordination networks.<sup>15</sup> Such applicability was demonstrated in 1994 with the synthesis of a two-dimensional square network solid  $[\text{Cd}(4,4'\text{-bpy})_2(\text{NO}_3)_2]$  containing large cavities with the possibility of guest encapsulation (Scheme 1.6a).<sup>16</sup> Crucially, the first catalytic process within a porous coordination network was demonstrated by treating benzaldehyde and cyanotrimethylsilane with a  $\text{CH}_2\text{Cl}_2$  suspension of powdered  $[\text{Cd}(4,4'\text{-bpy})_2(\text{NO}_3)_2]$  ( $40^\circ\text{C}$ , 24 h), which gave 2-(trimethylsiloxy)phenylacetonitrile in 77% yield (Scheme 1.6b). Later on, we reported the cyanosilylation of imines catalyzed by  $[\text{Cd}(4,4'\text{-bpy})_2(\text{H}_2\text{O})_2](\text{NO}_3)_2 \cdot 4\text{H}_2\text{O}$  (Scheme 1.6c).<sup>17</sup>



SCHEME 1.6

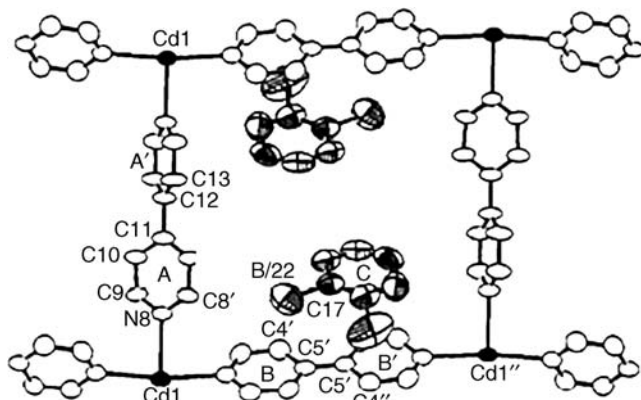


**FIGURE 1.6** View of the complex  $[\text{Cd}(\text{bpy})_2](\text{NO}_3)_2(\text{C}_6\text{H}_4\text{Br}_2)_2$  showing 50% probability ellipsoids. Nitrate ions have been omitted for clarity.

The ability to include guest molecules within the cavities was observed by preparation of a clathrate with *o*-dibromobenzene. The inclusion of the aromatic guest was confirmed by single-crystal X-ray diffraction. The structure was described as a graphite-like stacking of two-dimensional layers on top of each other (i.e., interplanar distance *ca.* 6.30 Å). One layer consists of an edge-sharing, perfectly planar square with a Cd(II) ion and 4,4'-bpy at each corner and side, respectively. Two *o*-dibromobenzene are included in each square void (Figure 1.6).

At the almost same time, Zaworotko and Yaghi reported organic coordination networks in 1995.<sup>18,19</sup> Zaworotko and coworkers reported the formation of a coordination network  $[\text{Zn}(4,4'\text{-bpy})_2]\text{SiF}_6$  with large non-interpenetrated channels (Figure 1.7). The effective pore size ( $8 \times 8 \text{ \AA}^2$ ) is comparable to the pore sizes of

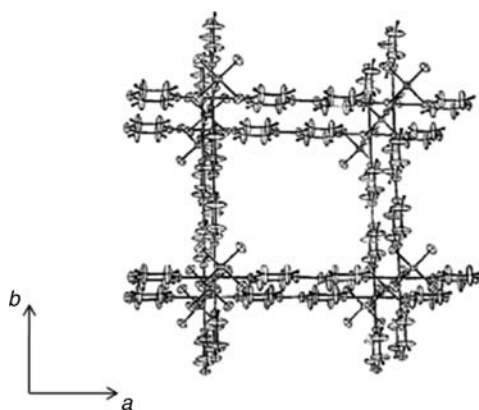


**FIGURE 1.7** ORTEP representation of a square channel viewed along the *c* crystallographic axis. The dimensions of the channels are the same as the dimensions of the unit cell *ca.*  $11.396 \times 11.396 \text{ \AA}^2$ .

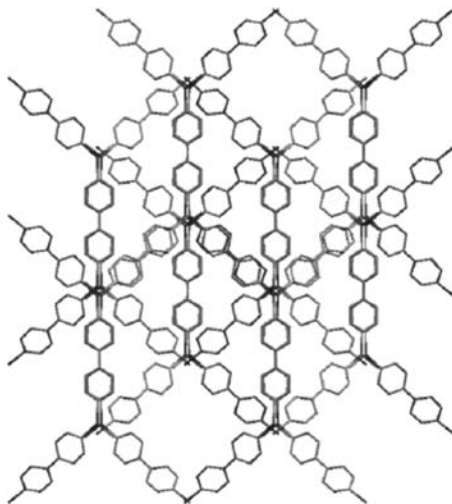


**FIGURE 1.8** Crystal structure of  $[\text{Cu}(4,4'\text{-bpy})_{1.5}](\text{NO}_3)\cdot(\text{H}_2\text{O})_{1.25}$  viewed along the  $[100]$  crystallographic direction. Nitrate anions and water molecules have been omitted for clarity.

large zeolites. The volume corresponding to the pores is about the 50% of the total volume. Interestingly, the pores are hydrophobic, which, in principle, should be able to include hydrophobic molecules with dimensions in the order of the pore size.

In the same year, Yaghi and coworkers succeeded on the hydrothermal synthesis preparation of another coordination network containing three identical interpenetrated channels. Single-crystal X-ray diffraction revealed the extended network of  $[\text{Cu}(4,4'\text{-bpy})_{1.5}]\text{NO}_3(\text{H}_2\text{O})_{1.25}$  in which trigonal planar  $\text{Cu}^{\text{I}}$  centers are linked by rod-like 4,4'-bpy ligands forming an extended 3D porous network (Figure 1.8). The interpenetrated networks did not fill all the available space as observed in many other solids, therefore leaving an important volume of the solid as rectangular channels. Those channels are filled with nitrate anions and water molecules and are linked by hydrogen bond interactions. Ion exchange properties were investigated. Nitrate ions were replaced in aqueous solutions with other ions such as  $\text{SO}_4^{2-}$  and  $\text{BF}_4^-$ . Under inert atmosphere, the coordination network was observed to be stable up to  $180^\circ\text{C}$  and for hours in water at  $70^\circ\text{C}$ .

The synthesis and crystal structures of new porous coordination networks with gas adsorption properties were first reported by Kitagawa and coworkers in the late 1990s.<sup>20</sup> Three structures  $[\text{M}_2(4,4'\text{-bpy})_3(\text{NO}_3)_4](\text{H}_2\text{O})_x$  (where  $\text{M} = \text{Co}, \text{Ni}, \text{and Zn}$ ) were characterized by X-ray crystallography. The coordination network with Co metal was determined by single-crystal X-ray diffraction, and the isomorphous porous coordination networks with Ni and Zn metals were demonstrated by powder X-ray diffraction (Figure 1.9). These solids have two channels running parallel to the  $b$  and  $c$  crystallographic axes whose dimensions are  $3 \times 6$  and  $3 \times 3 \text{ \AA}^2$ , respectively. The channels are filled with water molecules that are not bonded to the crystal framework.

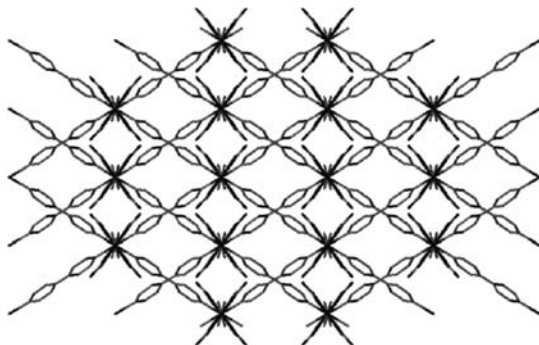


**FIGURE 1.9** Crystal structure corresponding to  $[\text{Co}_2(4,4'\text{-bpy})_3](\text{NO}_3)_4 \cdot (\text{H}_2\text{O})_4$  viewed along the  $c$ -axis. Hydrogen atoms have been omitted for clarity.

Gas-adsorption properties were studied due to the 3D porous nature of such coordination network. Under dried vacuum, the adsorption activity for  $\text{CH}_4$ ,  $\text{N}_2$ , and  $\text{O}_2$  was investigated. Clearly, diffusion of the different gases was observed (Figure 1.10). For 1 g of the anhydrous sample at 30 atm, about 2.3 mmol of  $\text{CH}_4$  and 0.80 mmol of  $\text{N}_2$  or  $\text{O}_2$  were adsorbed. Importantly, powder X-ray diffraction confirmed that during the gas adsorption process there was no loss of crystallinity.

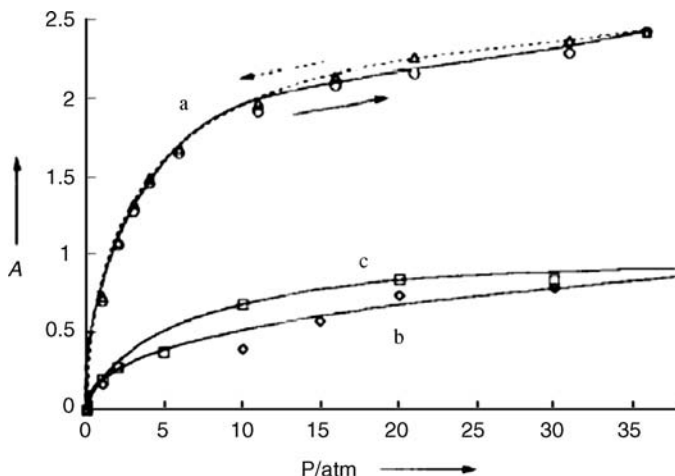


**FIGURE 1.10** Isotherms showing the adsorption of  $\text{CH}_4$  (a),  $\text{N}_2$  (b), and  $\text{O}_2$  (c) carried at room temperature for  $[\text{Co}_2(4,4'\text{-bpy})_3](\text{NO}_3)_4 \cdot (\text{H}_2\text{O})_4$  in the range of 1–36 atm. For the  $\text{CH}_4$  gas desorption (circles) was carried out directly after gas adsorption (triangles). The similarity between the two curves denotes that there are no structural changes during the adsorption process.



## 1.5 SINGLE-CRYSTAL-TO-SINGLE-CRYSTAL PHENOMENA IN POROUS COORDINATION NETWORKS

After application to catalysis, our interests moved on to single-crystal-to-single-crystal phenomena (SCSC), because organic coordination networks often crystallize very well. Crystallographic studies are useful as they provide valuable information about the relative atomic and molecular positions within a crystalline solid. In this regard, detailed information can be obtained from SCSC transformations. For instance, such solid-state processes enable one to analyze framework transformations and molecular interactions between guest-guest and host-guest within the pores in detail.<sup>21</sup>

### 1.5.1 SCSC Guest Removal

The first successful SCSC guest removal was reported by Kepert in 2000.<sup>22</sup> They prepared  $[\text{Ni}_2(4,4'\text{-bpy})_3](\text{NO}_3)_4 \cdot 6\text{EtOH}$ . The interlocked bilayer framework has  $6 \times 3 \text{ \AA}^2$  channels, which can reversibly uptake  $\text{H}_2\text{O}$  at room temperature with other guests such as EtOH, MeOH, and *i*-PrOH (Figure 1.11). The desolvation process at  $100^\circ\text{C}$  causes just a 2.4% decrease in cell volume and the mosaicity of the crystal remains intact.

### 1.5.2 SCSC Framework Dynamics

Unlike zeolite, one of salient features of organic coordination networks is their flexible frameworks capable of SCSC drastic framework transformation. We reported in 2000 the synthesis of an open  $20 \times 20 \text{ \AA}^2$  square-grid coordination network.  $[\text{Ni}(4,4'\text{-bis}(4\text{-pyridyl})\text{biphenyl})_2](\text{NO}_3)_2 \cdot 4(o\text{-xylene})$  was prepared via self-assembly of a rod-like ligand, 4,4'-bis(4-pyridyl)biphenyl, with  $\text{Ni}(\text{NO}_3)_2$  in *o*-xylene.<sup>23</sup> The framework has remarkable thermal stability and maintains its integrity up to  $300^\circ\text{C}$ . SCSC sliding of 2D-coordination layers of  $[\text{Ni}(4,4'\text{-bis}(4\text{-pyridyl})\text{biphenyl})_2](\text{NO}_3)_2 \cdot 4(o\text{-xylene})$ <sup>24</sup> triggered by guest exchange was successfully observed by X-ray analysis (Figure 1.12).<sup>25</sup> The crystals of  $[\text{Ni}(4,4'\text{-bis}(4\text{-pyridyl})\text{biphenyl})_2](\text{NO}_3)_2 \cdot 4(o\text{-xylene})$  showed guest specificity and exchanges of *o*-xylene for mesitylene but not for *m*-xylene, or 1,3- or 1,2-dimethoxybenzene. The crystals of a mesitylene-inclusion network,  $[\text{Ni}(4,4'\text{-bis}(4\text{-pyridyl})\text{biphenyl})_2](\text{NO}_3)_2 \cdot 1.7(\text{mesitylene})$ , were prepared by immersion of  $[\text{Ni}(4,4'\text{-bis}(4\text{-pyridyl})\text{biphenyl})_2](\text{NO}_3)_2 \cdot 4(o\text{-xylene})$  in mesitylene for 6 h. The single-crystal analysis of  $[\text{Ni}(4,4'\text{-bis}(4\text{-pyridyl})\text{biphenyl})_2](\text{NO}_3)_2 \cdot 1.7(\text{mesitylene})$  revealed considerable sliding of the layers relative to the 2D-framework of  $[\text{Ni}(4,4'\text{-bis}(4\text{-pyridyl})\text{biphenyl})_2](\text{NO}_3)_2 \cdot 4(o\text{-xylene})$  (Figure 1.13). Edge-to-face aromatic interactions exist at the corner of the channels in both  $[\text{Ni}(4,4'\text{-bis}(4\text{-pyridyl})\text{biphenyl})_2](\text{NO}_3)_2 \cdot 4(o\text{-xylene})$  and  $[\text{Ni}(4,4'\text{-bis}(4\text{-pyridyl})\text{biphenyl})_2](\text{NO}_3)_2 \cdot 1.7(\text{mesitylene})$  but not along the walls. The dimensions of the channels in  $[\text{Ni}(4,4'\text{-bis}(4\text{-pyridyl})\text{biphenyl})_2](\text{NO}_3)_2 \cdot 1.7(\text{mesitylene})$  are much bigger than those of  $[\text{Ni}(4,4'\text{-bis}(4\text{-pyridyl})\text{biphenyl})_2](\text{NO}_3)_2 \cdot 4(o\text{-xylene})$ . The sliding motion of the 2D-layers could be monitored by X-ray powder and single-crystal diffraction. The crystallographic results and GC analysis clearly indicate that the framework

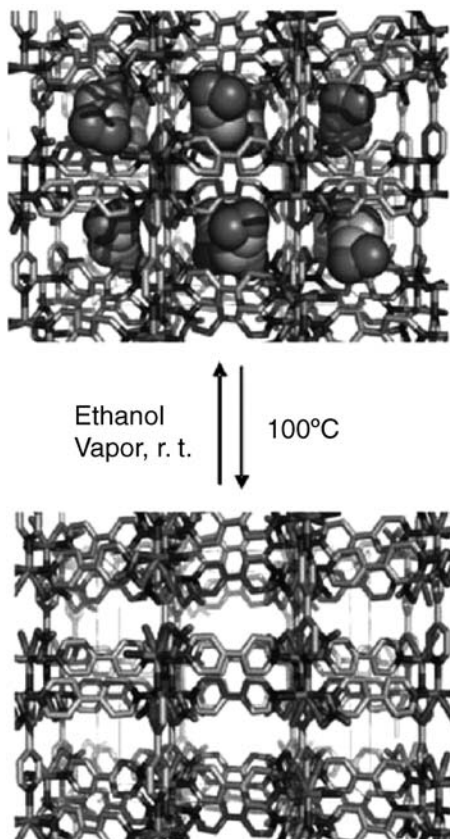


**FIGURE 1.11** Guest inclusion/removal in  $[\text{Ni}_2(4,4'\text{-bpy})_3](\text{NO}_3)_4 \cdot 6\text{EtOH}$  viewed down the  $a$ -axis. Ethanol molecules (space-filling model) are disordered.

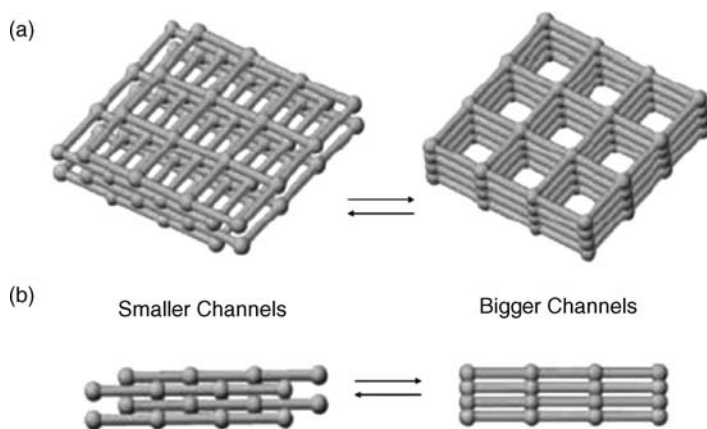


**FIGURE 1.12** Sliding motion of 2D-layers: (a) top and (b) side views.

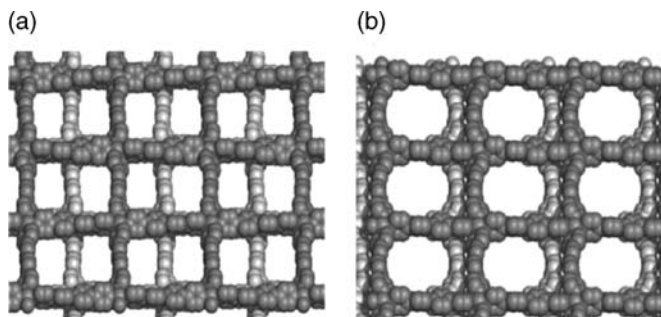


**FIGURE 1.13** Packing of 2D layers viewed along the  $c$ -axis in (a)  $[\text{Ni}(4,4'\text{-bis}(4\text{-pyridyl})\text{biphenyl})_2](\text{NO}_3)_2 \cdot 4(o\text{-xylene})$  4 and (b)  $\text{Ni}(4,4'\text{-bis}(4\text{-pyridyl})\text{biphenyl})_2(\text{NO}_3)_2 \cdot 1.7(\text{mesitylene})$ . Solvent molecules are omitted for clarity.

transformation proceeds in a crystal-to-crystal fashion. The first step is guest exchange, and the second step is the sliding of the layers.

Two years later, in 2002, Suh and coworkers also reported SCSC dynamic framework transformation.<sup>26</sup> They prepared a coordination porous bilayer-open-framework (BOF-1),  $[\text{Ni}_2(\text{C}_{26}\text{H}_{52}\text{N}_{10})]_3[\text{BTC}]_4 \cdot 6\text{C}_5\text{H}_5\text{N} \cdot 36\text{H}_2\text{O}$ , which was synthesized from the reaction of dinickel(II) bismacrocylic complex  $[\text{Ni}_2(\text{C}_{26}\text{H}_{52}\text{N}_{10})(\text{Cl})_4] \cdot \text{H}_2\text{O}$  and sodium 1,3,5-benzenetricarboxylate ( $\text{Na}_3\text{BTC}$ ) in water in the presence of DMSO and pyridine.

X-ray diffraction revealed two-dimensional layers formed between the Ni(II) macrocyclic unit and the  $\text{BTC}^{3-}$  ions are separated by the  $p$ -xylyl groups that act as pillars (Figure 1.14).

The coordination network has 3D channels with an effective channel width of *ca.* 11.12 Å (Figure 1.14 top) that are filled with water and pyridine molecules. The void volume corresponding to the channels was estimated to be 61% of the total volume. Upon exposure of  $[\text{Ni}_2(\text{C}_{26}\text{H}_{52}\text{N}_{10})]_3[\text{BTC}]_4 \cdot 6\text{C}_5\text{H}_5\text{N} \cdot 36\text{H}_2\text{O}$  at 75°C for 1.5 h, all the aromatic and nearly all water molecules were removed to yield  $[\text{Ni}_2(\text{C}_{26}\text{H}_{52}\text{N}_{10})]_3[\text{BTC}]_4 \cdot 4\text{H}_2\text{O}$ . Despite the significant structural reorganization (i.e., the cell volume changed from 5974.3 to 3877.9 Å<sup>3</sup>) the crystallinity was maintained. It was observed by X-ray diffraction that the thickness of the bilayer was reduced considerably due to the tilting of the  $p$ -xylyl molecules (Figure 1.14 bottom). Interestingly, powder X-ray diffraction revealed that the process is reversible when  $[\text{Ni}_2(\text{C}_{26}\text{H}_{52}\text{N}_{10})]_3[\text{BTC}]_4 \cdot 4\text{H}_2\text{O}$  was immersed in a solution containing water and pyridine during only 5 min.

### 1.5.3 Robust Hydrogen-Bonded 2D-Grid Network

In 2005, we reported a robust 2D-grid network considerably stabilized by hydrogen bonding.<sup>27</sup> The bidentate bridging ligand was simply modified by introducing ethylene glycol chains as hydrogen bonding sites. The modification of the link enabled us to perform the *in situ* crystallographic observation of reversible apical ligand

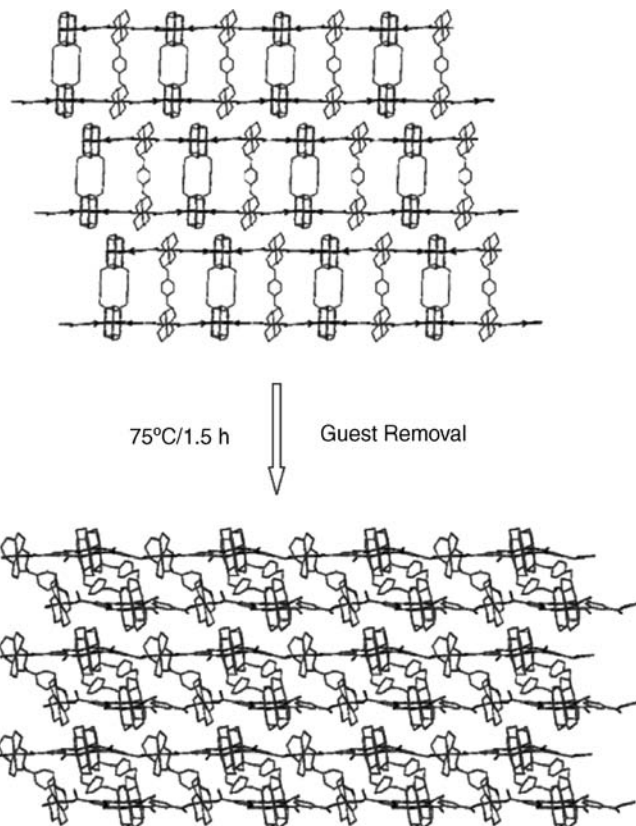
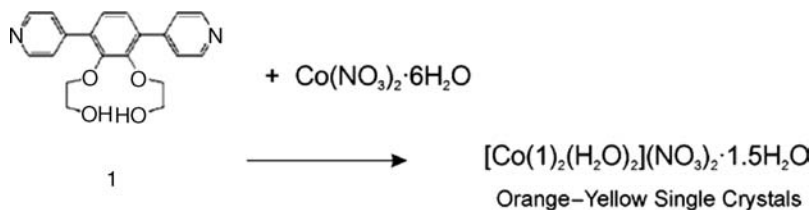


**FIGURE 1.14** X-ray structures of BOF-1. View of  $[\text{Ni}_2(\text{C}_{26}\text{H}_{52}\text{N}_{10})_3][\text{BTC}]_4 \cdot 6\text{C}_5\text{H}_5\text{N} \cdot 36\text{H}_2\text{O}$  along the  $a$ -axis (top). View along the  $b$ -axis of  $[\text{Ni}_2(\text{C}_{26}\text{H}_{52}\text{N}_{10})_3][\text{BTC}]_4 \cdot 4\text{H}_2\text{O}$  showing the tilting of the  $p$ -xylyl groups as a consequence of the water loss (bottom). Water and pyridine molecules have been omitted for clarity.

exchange at a cobalt center at  $150^\circ\text{C}$ . It was shown how the aqua and nitrate ligands can be reversibly coordinated to the cobalt center in a SCSC fashion.

A rod-like pyridyl ligand containing ethylene glycol side chains (**1**) was synthesized (Scheme 1.7). Slow complexation of  $\text{Co}(\text{NO}_3)_2 \cdot 6\text{H}_2\text{O}$  in MeOH over a solution



2

SCHEME 1.7

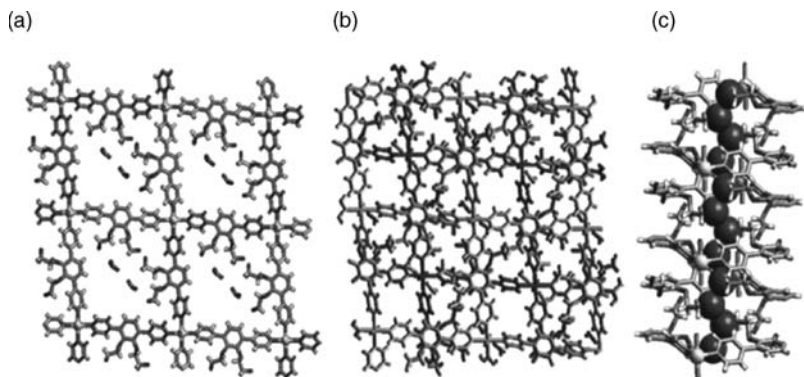


**FIGURE 1.15** (a) Square-rigid network of  $[\text{Co}(\mathbf{1})_2(\text{H}_2\text{O})_2](\text{NO}_3)_2 \cdot 1.5\text{H}_2\text{O}$ . Guest molecules ( $\text{H}_2\text{O}$ ) have been omitted for clarity. (b) The two-layer stack of **2**. (c) The infinite 1D hydrogen bonding interaction ( $\text{O}-\text{H} \cdots \text{O}$ ) between layers in  $[\text{Co}(\mathbf{1})_2(\text{H}_2\text{O})_2](\text{NO}_3)_2 \cdot 1.5\text{H}_2\text{O}$ . The oxygen atoms of the hydroxyl groups are represented by a space-filling model.

of **1** in toluene produced orange–yellow single crystals of  $[\text{Co}(\mathbf{1})_2(\text{H}_2\text{O})_2](\text{NO}_3)_2 \cdot 1.5\text{H}_2\text{O}$  (**2**).

Crystallographic analysis revealed the formation of square-grid network structure where the grid sheet layers are stacked on top of each other (Figure 1.15a). The two layers are in an offset fashion on both edges (Figure 1.15b). Interestingly, the ethylene glycol chains play two important roles. First, they add considerable stabilization to the crystal due to 1D hydrogen-bond ( $\text{O}-\text{H} \cdots \text{O}$ ) arrays that interpenetrate the layers (Figure 1.15c). Second, they also introduce moderate flexibility within the cavity by allowing guest molecules to behave as in a solution-like environment. In fact, a similar square-grid coordination network without functionalized bridging ligands gradually deteriorated above room temperature due to the loss of guest molecules. Importantly, the increased stability and flexibility of  $[\text{Co}(\mathbf{1})_2(\text{H}_2\text{O})_2](\text{NO}_3)_2 \cdot 1.5\text{H}_2\text{O}$  allowed us to directly observe a reversible apical-ligand-exchange reaction at the hinge metals by single-crystal X-ray crystallography.

Two water molecules are coordinated to the cobalt(II) center at the apical positions (aqua form) with four pyridyl groups at the equatorial positions (Figure 1.16a). Upon heating at  $150^\circ\text{C}$  a single crystal of  $[\text{Co}(\mathbf{1})_2(\text{H}_2\text{O})_2](\text{NO}_3)_2 \cdot 1.5\text{H}_2\text{O}$  during 1 day, the yellow crystal turned red without loss of crystallinity. Crystallographic analysis revealed that the apical water molecules were substituted by two nitrate ions and extruded from the crystal to form the nitrate complex  $[\text{Co}^{\text{II}}(\mathbf{1})_2(\text{NO}_3)_2]$  (Figure 1.16b). It was observed that after leaving  $[\text{Co}^{\text{II}}(\mathbf{1})_2(\text{NO}_3)_2]$  at room temperature, it returned to the initial aqua form. The crystal changed from red to yellow in color and the crystallinity was maintained. Crystallographic and elemental analysis showed that the new obtained aqua form  $[\text{Co}(\mathbf{1})_2(\text{H}_2\text{O})_2](\text{NO}_3)_2 \cdot 1.5\text{H}_2\text{O}$  is almost identical to the original structure of  $[\text{Co}(\mathbf{1})_2(\text{H}_2\text{O})_2](\text{NO}_3)_2 \cdot 1.5\text{H}_2\text{O}$  (Figure 1.16c).

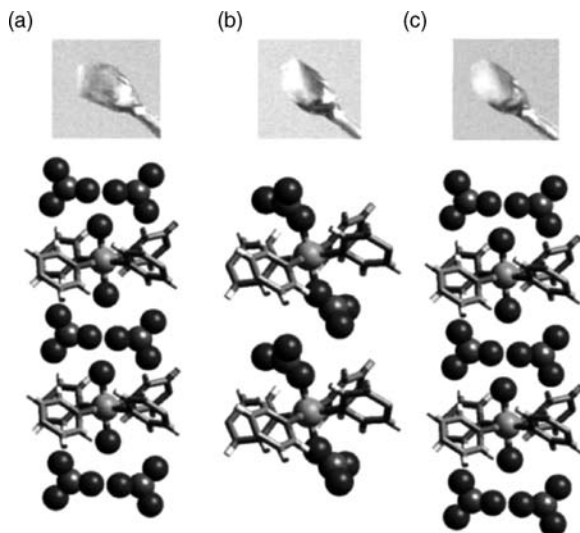


**FIGURE 1.16** Photographs corresponding to the actual crystals and molecular structures around the cobalt ion: (a) original crystal  $[\text{Co}(\mathbf{1})_2(\text{H}_2\text{O})_2](\text{NO}_3)_2 \cdot 1.5\text{H}_2\text{O}$ , (b) the crystal after heating at  $150^\circ\text{C}$  for 24 h  $[\text{Co}^{\text{II}}(\mathbf{1})_2(\text{NO}_3)_2]$ , and (c) the crystal after exposure of  $[\text{Co}^{\text{II}}(\mathbf{1})_2(\text{NO}_3)_2]$  to air  $[\text{Co}(\mathbf{1})_2(\text{H}_2\text{O})_2](\text{NO}_3)_2 \cdot 1.5\text{H}_2\text{O}$ . Two other disordered nitrate ions have been omitted for clarity.

## 1.6 EXPANSION FROM TWO- TO THREE-WAY LINK: CONSTRUCTION OF TPT COORDINATION NETWORKS

Self-assembly of a two-way link with metal ion connectors provides predictable architecture. What about a three-way link? The triazine ligand 2,4,6-tris(4-pyridyl)-triazine (TPT) was chosen as a three-way link. In fact, a three-way link of TPT gives more variety of discrete coordination cages having a large void capable of encapsulating hydrophobic guests. We reported molecular  $\text{M}_6\text{L}_4$  cages (M: *cis*-protected Pd or Pt; L: TPT) in 1995.<sup>28</sup> Meanwhile we attempted to prepare coordination networks consisting of metal ions and TPT, but had no success.

In 1996, Robson and coworkers succeeded in the preparation of a TPT coordination network.<sup>29</sup> A porous coordination network in which two independent cubic nets are interpenetrated was synthesized by diffusion of a solution of  $[\text{Cu}(\text{CH}_3\text{CN}_4)]\text{ClO}_4$  in acetonitrile into a solution of TPT in  $\text{CHCl}_3/1,1,2,2$ -tetrachloroethane. Dark red crystals of  $[\text{Cu}_3(\text{TPT})_4](\text{ClO}_4)_3$  were analyzed by single-crystal X-ray diffraction.

The repeating structural unit in the network is formed by six Cu centers at the corners of a regular octahedron. Large octahedral chambers are formed in which each chamber is connected through six Cu metal vertices to six others (Figure 1.17). An infinite arrangement of cubic chambers is then produced. At the center of each collection of eight chambers, there is a cavity that can accommodate a chamber of an independent but identical infinite network (Figure 1.18). Importantly, the octahedral chambers are left unoccupied, which generates a solid with large empty voids that can include other molecules.